

We are IntechOpen, the world's leading publisher of Open Access books Built by scientists, for scientists

6,900

Open access books available

186,000

International authors and editors

200M

Downloads

Our authors are among the

154

Countries delivered to

TOP 1%

most cited scientists

12.2%

Contributors from top 500 universities



WEB OF SCIENCE™

Selection of our books indexed in the Book Citation Index
in Web of Science™ Core Collection (BKCI)

Interested in publishing with us?
Contact book.department@intechopen.com

Numbers displayed above are based on latest data collected.
For more information visit www.intechopen.com



Optimizing Processing Conditions to Produce Cobalt Ferrite Nanoparticles of Desired Size and Magnetic Properties

Oscar Perales-Pérez and Yarilyn Cedeño-Mattei

Additional information is available at the end of the chapter

<http://dx.doi.org/10.5772/66842>

Abstract

The excellent chemical stability, good mechanical hardness, and a large positive first order magnetocrystalline anisotropy constant of cobalt ferrite (CoFe_2O_4) make it a promising candidate for magneto-optical recording media. For practical applications, the capability to control particle size at the nanoscale is required in addition to precise control of the composition and structure of CoFe_2O_4 . It has been well established that a fine tuning in cobalt ferrite nanocrystal size within the magnetic single domain region would lead to the achievement of extremely high coercivity values at room temperature. The development of a size-sensitive phase separation method for cobalt ferrite that is based on a selective dissolution of the superparamagnetic fraction and subsequent size-sensitive magnetic separation of single-domain nanoparticles is presented. The attained room temperature coercivity value (11.9 kOe) was mainly attributed to the enlargement of the average crystal size within the single domain region coupled with the removal of the superparamagnetic fraction. The strong influence of crystal size, ferrite composition, and cation distribution in the ferrite lattice on the corresponding magnetic properties at the nanoscale was also confirmed. The superparamagnetic and magnetic single domain limits were experimentally determined.

Keywords: cobalt ferrite, nanocrystals, size-controlled synthesis, high coercivity, magnetic properties

1. Introduction

Technological applications of cobalt ferrite (CoFe_2O_4) nanocrystals include their potential use in ferrofluids, hyperthermia, and biological treatment agents due to their unusual properties

[1, 2]. In addition, CoFe_2O_4 possesses excellent chemical stability, good mechanical hardness, and a large positive first order crystalline anisotropy constant, making it a promising candidate for magneto-optical recording media also [3]. Control on particle size and shape, ion distribution, and/or structure could allow a fine-tuning of the magnetic properties of ferrites [4–7]. In this regard, magnetic nanocrystals exhibit strong size-dependent properties that may provide valuable information on estimating the scaling limits of magnetic storage while contributing to the development of high-density data storage devices.

To the best of our knowledge, there is still a lack of a systematic effort to restrict the growth of single nanocrystals within the magnetic single domain region where enhancement of coercivity could be achieved. Theoretically, the single domain region ranges between 5 and 40 nm [8]. Maximum coercivity value of around 5.3 kOe [9] has also been reported for 40 nm nanocrystals. Since coercivity is strongly dependent on particle size, any attempt to achieve higher coercivity values in cobalt ferrite must consider the development of alternative approaches in order to obtain more homogeneous crystal sizes with less or null presence of superparamagnetic particles, which have near-zero coercivity.

It is desired to select a synthesis procedure capable of producing nanocrystals with a narrow size distribution due to the above-mentioned direct dependence of coercivity on crystal size. Synthesis approaches such as reverse micelles and thermal decomposition meet this criterion but the excessive consumption of resources, namely, synthesis reagents and experimental time, must be minimized. The use of toxic solvents and surfactants make these processes less attractive. On the other hand, aqueous-based synthesis routes (e.g., coprecipitation method) are environmentally friendly; the experimental time and reagents consumption are minimum and, most important, can allow a fine-tuning of crystal size.

Although coercivity is mainly governed by the magnetocrystalline anisotropy energy, contribution from surface anisotropy becomes important, particularly on the nanoscale. Additionally, the strain anisotropy and shape anisotropy as well as the ferrite composition will also contribute to the magnetic anisotropy and superexchange interaction energies.

Based on the above considerations, the present chapter addresses the experimental optimization of the synthesis parameters leading to the precise control of the coercivity of cobalt ferrite nanocrystals. In particular, the systematic study on composition, size, and cation distribution allowed the determination of the experimental limits of the single and multidomain regions as a function of the ferrite crystal size.

2. Theoretical background

2.1. Ferrites

The spinel structure derives from the mineral MgAl_2O_4 whose structure was elucidated in 1915. Analogous to it, the spinel structure in ferrites has the general formula MFe_2O_4 , where M corresponds to a divalent metal (i.e. Co^{2+} , Mn^{2+} , Ni^{2+} , and Zn^{2+}). The spinel lattice [10] is composed of a close-packed oxygen arrangement with 32 oxygen atoms forming the unit

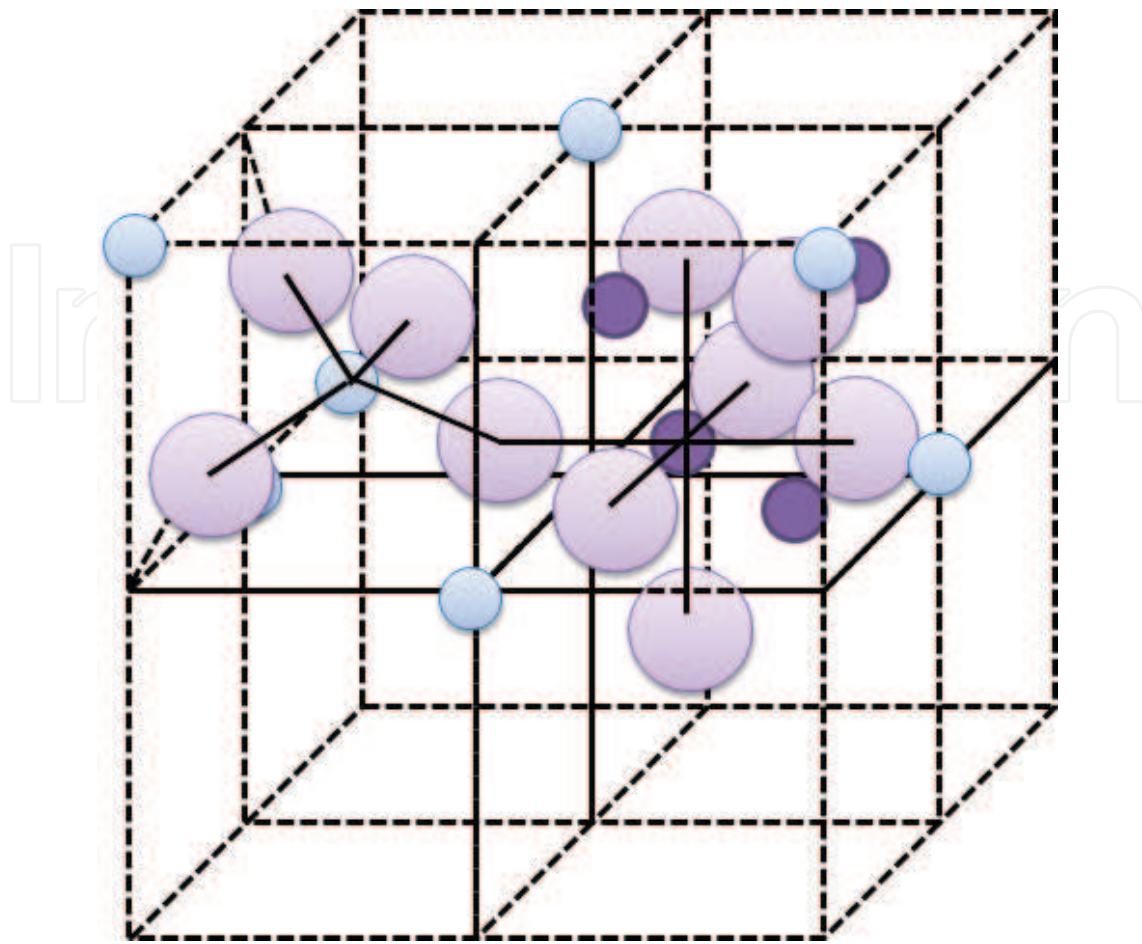


Figure 1. The spinel structure [10].

cell and includes two types of atomic arrangements, called A and B sites, where the cations are accommodated. The site A is tetrahedrally and the B site is octahedrally coordinated by oxygen atoms; the spinel unit cell contains 64 tetrahedral sites, only 8 being occupied, and 32 octahedral sites, with half of them occupied. More specifically, a spinel unit cell can be considered to consist of two types of subcells (**Figure 1**) that alternate in a three-dimensional array. The magnetic properties exhibited by this kind of structures are also influenced by the interaction of cations on the A and B sites; for instance, large angles and short distances between cations would be conducive to the enhancement of the exchange coupling and hence to the corresponding magnetic properties. The angles in the spinel structure for the A-A, B-B, and A-B interactions are 79.63° , $90^\circ/125.3^\circ$, and $125.15^\circ/154.57^\circ$, respectively, thus A-B exchange interactions are the strongest.

2.2. The cobalt ferrite

Cubic ferrites could be classified as normal, inverse, or mixed spinels. In the case of a normal spinel, the divalent ions occupy all the tetrahedral sites, whereas the trivalent ions do the same with the octahedral sites. An example of a material with a normal spinel structure is ZnFe_2O_4 . In the case of inverse spinels such as cobalt ferrite, all tetrahedral sites are occupied

by the trivalent ion (Fe^{3+}) whereas octahedral sites are equally occupied by divalent (Co^{2+}) and trivalent ions (Fe^{3+}) [11]. The magnetic moment = $5 \mu_B$ from octahedral Fe^{3+} ions is antiparallel to the magnetic moment = $5 \mu_B$ from the tetrahedral Fe^{3+} ions, thus compensating each other. Accordingly, the magnetization in cobalt ferrite is attributed to the magnetic moment = $3 \mu_B$ provided by Co^{2+} ions on the B-sites.

2.3. Magnetic properties and particle size

There is a relationship between coercivity and particle size [12] that is based on the presence of magnetic domains. Magnetic particles would behave as single domain (SD) or multidomain (MD) depending on particle size (as seen in **Figure 2**). This SD region is subdivided into two main regions characterized by their magnetic stability and they are known as the unstable and the stable regions. The unstable region corresponds to the superparamagnetic particles (SPM). It is a size-dependent issue where the thermal energy overcomes the anisotropy energy causing the spins rotate and randomize acting as paramagnetic (do not retain magnetization and coercivity after magnetic field removal).

As seen in Eq. (1), the critical radius below which particles behave as a single domain can be calculated by [13, 14]:

$$r_c = \frac{9 (AK_u)^{\frac{1}{2}}}{\mu_0 M_s^2} \quad (1)$$

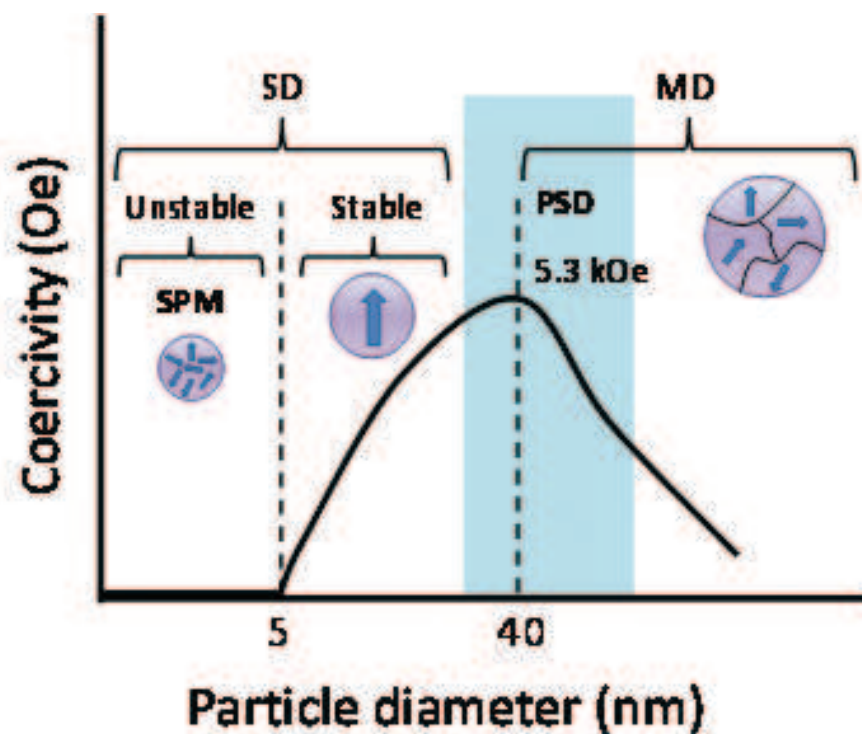


Figure 2. Dependence of coercivity with particle diameter for cobalt ferrite.

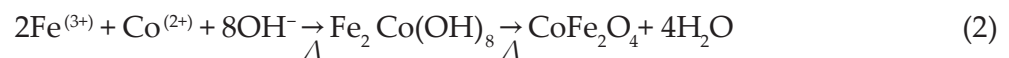
A is the exchange stiffness (constant characteristic of the material related to the critical temperature for magnetic ordering), K_u is the uniaxial anisotropy constant; μ_0 is the vacuum permeability, and M_s the saturation magnetization. For the stable single domain region, a simple model developed by Stoner and Wohlfarth [15] assumes coherent spin rotation whereby all spins within the single-domain particle are collinear (the magnetization is uniform) and rotate in unison. The model predicts the field strength necessary to reverse the spin orientation direction or coercivity. In this stable region, the magnetocrystalline energy gradually overcomes the thermal energy and becomes responsible for the increase in coercivity. The only way to magnetize a material is to rotate the spins, a process that involves high energies and, hence, high coercivity. Thus, SD grains are magnetically hard and have high coercivity and remanent magnetization. In the cobalt ferrite case, the limit between the single and multidomain has been established to be around 40 nm with an expected coercivity of 5.3 kOe at room temperature. For the multidomain region, domain walls are present and coercivity tends to decrease with an increase in particle size [15]. In turn, the magnetization process in a multidomain, particle is controlled by domain wall movement, which is an energetically easier process.

Based on the above considerations, a precise control on the particle size will allow a fine tuning of the magnetic properties at the nanoscale. In this regard, our modified coprecipitation method described here allows the required control in crystal size based on enhancement of the heterogeneous nucleation mechanism. Consequently, a control in nucleation and growth steps could be achieved, which are key points for crystal size control.

3. Methodology

3.1. Conventional coprecipitation method

All reagents used in the synthesis and treatment of cobalt ferrite nanocrystals were of analytical grade and used without further purification. Ferrite nanocrystals are synthesized by the conventional coprecipitation method. In the conventional approach, an aqueous solution containing Co (II) and Fe(III) ions was rapidly contacted with an excess of hydroxide (OH⁻) ions. The hydrolysis reaction in the presence of an excess of OH⁻ ions leads to the formation of a paramagnetic Fe-Co hydroxide, which undergoes dehydration and atomic rearrangement conducive to a ferrite structure with no need of further annealing, according to:



The nucleation rate is quite high at the beginning of the precipitation process whereas the excess of OH⁻ ions provides a net negative surface charge to the nuclei limiting their further growth and aggregation. Under these conditions, polydispersed particles of less than 30 nm in diameter are typically produced.

The reactant solution was mechanically stirred at 500 rpm and intensively heated to accelerate the dissolution/recrystallization stages involved with the ferrite formation. The intensive heating helped to reduce the reaction time dramatically. Cobalt ferrite nanocrystals were washed out with deionized water, dried at 80°C for 24 hours and characterized.

3.2. Modified coprecipitation method

In order to enhance the magnetic properties by controlling the nucleation and growth conditions of the ferrite crystals, the conventional coprecipitation route was modified by controlling the flow rate of addition of the metal ions solution to the alkaline one under intensive heating conditions. For this purpose, a microperistaltic pump with a precise control of flow rate was used.

3.3. Combined acid washing and magnetically assisted size-sensitive separation

3.3.1. Single acid washing process

In order to improve the monodispersity of the as-synthesized cobalt ferrite nanocrystals, they were contacted with HCl solution; it is expected that a higher solubility of the smaller particles when compared to the bigger sized ones, would lead to a narrow size distribution and, therefore, higher coercivity values. Also, the acidic treatment could remove the “magnetically dead” surface in remaining particles. On an experimental basis, the ferrite nanocrystals produced using the above described modified coprecipitation method were then treated with the acidic solution for 1 hour.

As-synthesized nanocrystals were first contacted with 10% v/v HCl solution for 30 minutes at a $\frac{0.1 \text{ g ferrite}}{10 \text{ mL acidicsolution}}$ ratio. At the end of this acid treatment stage, the recovered solids were dispersed in water and submitted for the magnetically assisted separation stage using a commercial N38 (field strength $\geq 1.2 \text{ T}$) neodymium permanent magnet. The particles suspension was contacted with the magnet for 2 minutes at the end of which, settled particles were separated from the suspended ones that remained in the supernatant. The solids in this supernatant represented the first fraction of the size-sensitive separation process. In turn, the magnetically settled particles were processed through the same water dispersion-magnetic separation cycle for two more times. The fractions corresponding to the solids recovered from their corresponding supernatants and the last sediment were submitted for structural and magnetic characterization.

3.3.2. Double acid washing process

Five grams of ferrite synthesized by the above indicated modified coprecipitation method was used in the size-sensitive phase separation process and characterization. The ferrite to acidic solution mass/volume ratio was the same as described in the previous section. After a first acid washing and size-sensitive separation, the settled fraction with the largest amount of particles was used as a starting material for a second size-sensitive separation cycle (second settled fraction in this case). This experimental procedure will be known as combined

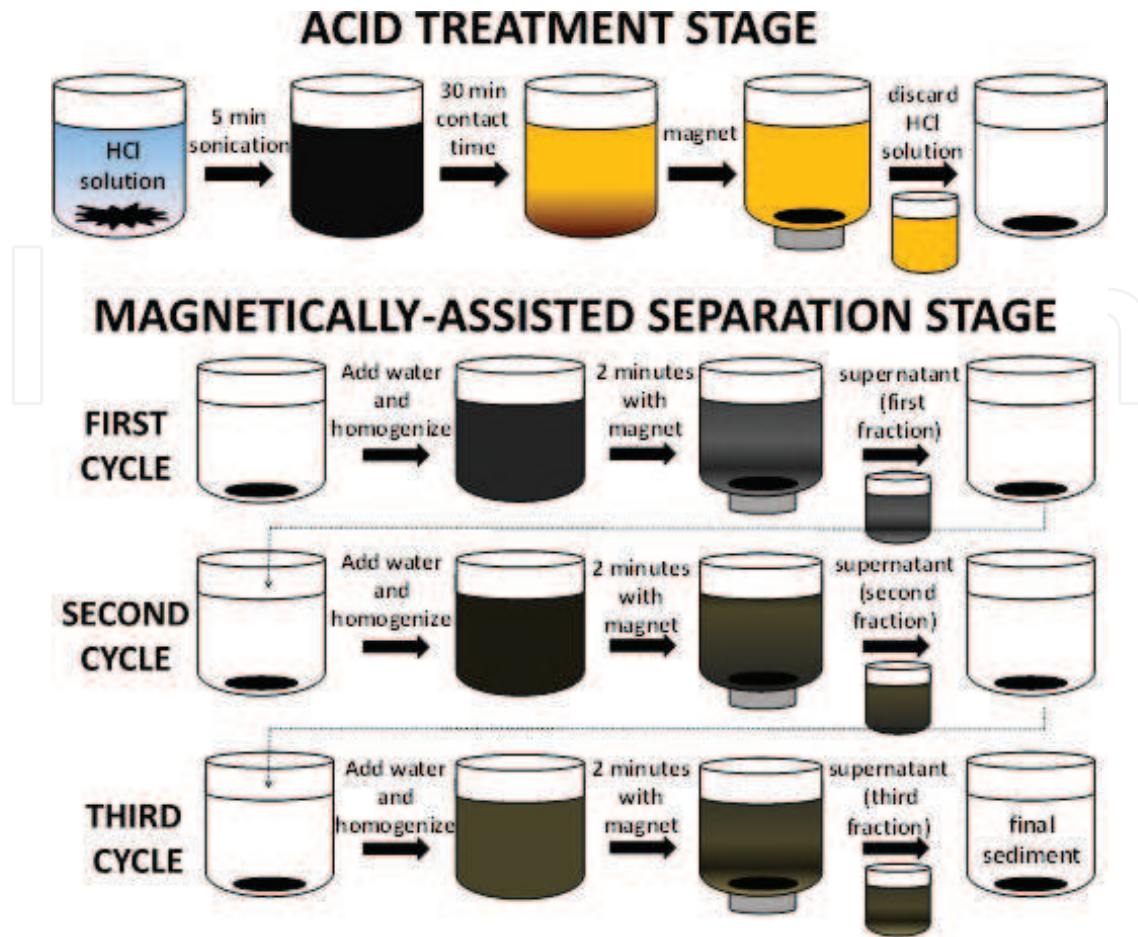


Figure 3. The acid washing and magnetically assisted size-sensitive separation.

acid washing and magnetically assisted size-sensitive separation (**Figure 3**), double acid washing process.

3.4. Effect of the ferrite composition: Variation of the Fe:Co mole ratio

Cobalt ferrite nanocrystals with initial Fe:Co mole ratios of 3:1, 2:1, 1.7:1, and 1.4:1 were produced by the conventional and the modified coprecipitation method (flow rate: 0.67 mL/min). The reaction time was kept constant at 1 hour.

3.5. Inhibition of crystal growth by using surfactants or polymers

As an attempt to determine the superparamagnetic limits in cobalt ferrite nanoparticles, oleic acid sodium salt (Na-oleate) was used in the synthesis of cobalt ferrite in order to inhibit crystal growth. This surfactant was introduced into the same vessel with the sodium hydroxide solution and heated as in the conventional coprecipitation method although for very short reaction times (5 minutes). Prolonged reaction times favored crystal growth. In a modified route, the boiling hydroxide and surfactant solution was removed from the heating source followed by its contact with the ionic solution containing iron (III) and cobalt (II).

4. Results and discussion

4.1. Optimization of synthesis parameters: 2³ Factorial design

The coprecipitation method employed in the synthesis of cobalt ferrite nanocrystals allows the manipulation of synthesis parameters such as reaction time (A), control on flow rate of the addition of reactants (B), and the NaOH concentration (C). A deep understanding of those parameters will allow a control in the nucleation and growth steps, key points in size-control approaches [8, 16, 17]. In order to increase coercivity, the superparamagnetic limit must be surpassed; this limit has been estimated at 5 nm [18].

It is important to take into account each parameter and the interactions between them in order to tune crystal size and hence, the magnetic properties. A 2³ factorial design is a useful tool in the study of the synthesis parameters and its interactions. The factorial design considers a low and a high level of each parameter under study. Each level was selected based on previous studies and taking into account the experimental limitations such as the capacity of the peristaltic pump used to control the flow rate of addition of reactants. The low and high levels for each parameter under study are summarized in **Table 1**. The levels were also coded using (-) and (+) signs for low and high, respectively.

In addition to the ABC Design, three replicates at the center of it were used to estimate the experimental error. **Table 1** also summarizes the response variable, i.e., coercivity. A wide range of coercivity values (between 870 and 4626 Oe) was obtained. The 2³ factorial design suggested that reaction time is not a significant parameter. Taking it into account, the reaction time was set to 1 hour in later experiments. Otherwise, the flow rate of addition of reactants, NaOH concentration, and the interaction between these two parameters are the most significant.

4.2. Combined acid washing and magnetically assisted size-sensitive separation

The modified size-controlled coprecipitation method to synthesize ferrite nanocrystals can allow a fine tuning of the average crystallite size within the single magnetic domain region.

Combinations	A B C Design	A: Reaction time (min)	B: Flow rate (mL/min)	C: NaOH (M)	H _c (Oe)
1	---	5	0.85	0.34	4518
A	+- -	180	0.85	0.34	4626
B	- + -	5	20	0.34	871
AB	++ -	180	20	0.34	870
C	-- +	5	0.85	0.54	2877
AC	+ - +	180	0.85	0.54	3448
BC	- ++	5	20	0.54	922
ABC	+++	180	20	0.54	1007

Table 1. Experimental conditions for the 2³ factorial design and the corresponding room temperature coercivity, H_c [19].

However, the product is still polydispersed in size [19]. Accordingly, any attempt to achieve higher coercivity values in cobalt ferrite must consider the development of an alternative approach in order to obtain more homogeneous crystal sizes with less or null presence of superparamagnetic particles. In this regard, a rapid and simple size-sensitive phase separation treatment based on the size-dependence of nanoparticles solubility in an aqueous phase was developed. In the case of particles with narrow size distribution, the dissolution behavior will depend on the ferrite degree of inversion and composition [20]. However, when moderately polydispersed nanocrystals are synthesized, the selective dissolution of tiny individual crystals can be expected according to the Ostwald-Freundlich law [21], i.e., particles with smaller diameter will be more soluble than bigger ones. This fact was taken into account to get rid of the superparamagnetic or smaller particles that do make the coercivity of the powders to decrease. The selective dissolution of superparamagnetic particles will be complemented by a magnetically assisted size-separation stage. The separation stage consists of contacting the nanoparticles/acid solution with a magnet in order to separate the settled particles from the suspended (smaller) ones.

4.2.1. Single acid washing process

The corresponding average crystallite size varied from 16 ± 2 nm in the as-synthesized sample to 22 ± 2 nm in the solid fraction recovered after 6 minutes of magnetic separation after treatment with 10% HCl solution. This enlargement of average crystallite size can be attributed to the preferential acidic dissolution of small nanoparticles including the superparamagnetic ones along with an efficient magnetically assisted size classification.

The full set of fractions recovered after treatment with 10% HCl solution is shown in **Figure 4**. The increment in crystal size with an increment in separation time is evident.

Transmission electron microscopy-energy dispersive spectroscopy (TEM-EDS) analyses were performed to measure the elemental composition and calculate the experimental Fe:Co mole ratio. TEM-EDS of cobalt ferrite nanocrystals suggested that selective dissolution of Fe could have taken place after contacting them with the 10% v/v HCl solution. The Fe:Co mole ratio decreased from 1.81:1 in the nontreated sample down to 1.58:1 after the acidic treatment. The selective dissolution of Fe in bulk ferrite was suggested by Figueroa et al. [22]; they attributed the drop in the Fe:Co ratio to the removal of the less crystalline surface layer of iron oxide in cobalt ferrite produced by thermal decomposition. As-synthesized particles show agglomeration while treated particles have better dispersion. It may be a result of electrostatic

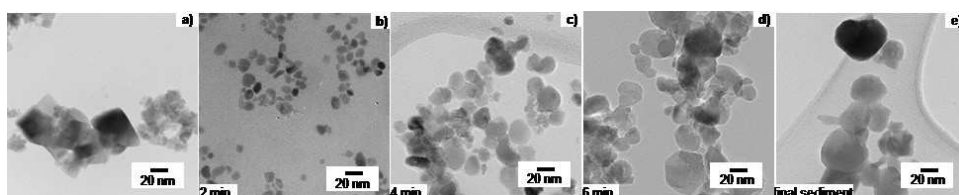


Figure 4. TEM images of CoFe_2O_4 powders before (a) and after acidic treatment with 10% HCl followed by magnetically assisted separation at different times (b–e). The images correspond to the solids contained in the fractions collected after 2 minutes (b), 4 minutes (c), and 6 minutes (d) of magnetic separation and the sediment at the end of this stage (e).

repulsion resulting from the chemisorption of charged species, in this case, H^+ , on the nanocrystal surfaces.

The coercivity of the as-synthesized ferrite powders was 5.4 kOe. It increased up to 9.4 kOe after treating the powders with 10% w/w HCl. The maximum magnetization of this high coercivity sample is 58 emu/g. The “constricted loops” observed in the central part of the M-H loops suggest a mixture of soft and hard material in the powders. In this case, the soft material corresponds to the superparamagnetic fraction. In turn, the large room temperature coercivity in these powders can be attributed to the enlargement of their average crystal size caused by the removal of the superparamagnetic fraction during the acidic treatment and the subsequent size-sensitive magnetic separation stages. This interpretation is supported by the results provided by TEM and XRD analyses on these samples. Furthermore, the reduction in the Fe:Co atomic ratio in the size-selected cobalt ferrite particles, suggested by TEM-EDS analyses, could also be involved with the drastic change in coercivity. In this case, acidic treatment should have promoted the removal of a poorly crystalline and magnetically disordered surface layer of the ferrite oxide.

Mössbauer spectra for the cobalt ferrite powders without treatment showed a broadened central peak, attributed to the presence of superparamagnetic particles, in addition to the hyperfine splitting typical of magnetically ordered iron species in the ferrite lattice. The relative abundance of the superparamagnetic portion was calculated at 19.3% while the combined three magnetically split sites accounted for 81.7% of the remainder of the cobalt ferrite. No central peak was observed in the Mössbauer spectrum for the sample recovered at the end of the magnetic separation stage, which suggest the complete removal of the superparamagnetic fraction after the acidic treatment and magnetic separation stages. The internal magnetic field for the first site, which was assigned to Fe in the tetrahedral site (Fe^{Tetra1}), was 449.97 kOe with quadrupole splitting of -1.584 mm/s and isomer shift of 1.087 mm/s, while its relative abundance was 29.1%. The other two sites corresponded to Fe in the octahedral ferrite sites (Fe^{Oct1}). The first one was characterized by the internal magnetic field of 481.13 kOe, quadrupole splitting of -0.974 mm/s and isomer shift of 0.024 mm/s with a relative abundance of 41.8%. The second octahedral site, Fe^{Oct2} , was fitted with an internal magnetic field of 391.31 kOe, quadrupole splitting of -0.640 mm/s, isomer shift of 0.085 mm/s, and relative abundance of 29.1%. The fittings are consistent with an inverse ferrite structure whereby Fe^{3+} cations randomly occupied both the tetrahedral and octahedral sites [23, 24]. Based on these considerations and since an equal occupation of the tetrahedral and octahedral sites by Fe^{3+} cations did not take place, an incomplete inversion in synthesized cobalt ferrite nanocrystals can be considered. This partial inversion in ferrite structure can also account for the unusual coercivity value.

4.2.2. The double acid washing process

As an attempt to explore the possibility of further enhancement of the ferrite coercivity by narrowing the size distribution even more, previously acid-washed ferrite powders were retreated by following a similar acid washing/magnetic separation cycles. Starting cobalt ferrite powders were synthesized by the modified coprecipitation method at 0.81 mL/min flow rate and a NaOH concentration of 0.315 M, which corresponds to the optimum concentration determined from the experimental design. A ferrite to acidic solution ratio of 5.0 g ferrite to

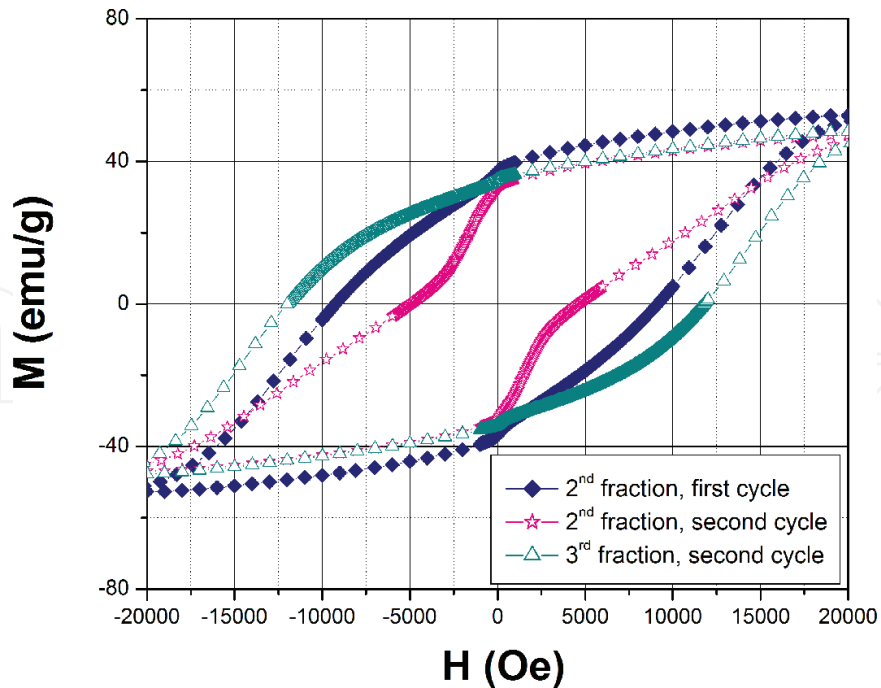


Figure 5. Room temperature M-H measurements of CoFe_2O_4 powders submitted to two cycles of acid treatment and magnetically assisted separation stages.

500 mL HCl 10% v/v was used. The coercivity increased starting from 3.3 up to 9.7 kOe for the third fraction after 6 minutes of magnetically assisted settling; this increment in coercivity is around three times its initial value. Again, “constricted” hysteresis loops were observed (Figure 5), which are typical of a mixture of soft and hard magnetic materials [25]. In this case, this sort of “necking” in the central part of the loop can be attributed to the coexistence of superparamagnetic single-domain cobalt ferrite nanoparticles. Fractions exhibiting larger coercivity values did not show this “necking” confirming the removal of the superparamagnetic fraction.

The second settled fraction (corresponding to 4 minutes of settling time) was submitted to the second cycle of our size-sensitive phase separation process. This time, the ferrite to HCl ratio was 0.8 g ferrite to 80 mL HCl 10% v/v. The sharpening in the corresponding XRD peaks suggested an improvement in crystallinity after the second treatment cycle.

The initially 9.2 kOe achieved in the second fraction generated during the first separation cycle was increased up to 11.9 kOe. This pretty large coercivity was obtained in the third fraction produced during the second acid washing/magnetic separation cycle. This dramatic enhancement in coercivity can be attributed to the larger crystal size in the corresponding fractions and a more efficient removal of any remaining superparamagnetic particles.

4.3. Effect of the ferrite composition

4.3.1. Variation of the Fe:Co mole ratio

The magnetic properties of cobalt ferrite depend on diverse factors such as crystal size [26], morphology [27], chemical composition [28, 29], and/or cation distribution [30]. The formation

of nonstoichiometric cobalt ferrite nanocrystals will lead to atomic rearrangement between A- and B-sites and/or creation of vacancies [31]. Consequently, a change in magnetic properties will take place. On this basis, cobalt ferrite nanocrystals with different initial Fe:Co mole ratios (3:1, 2:1, 1.7:1, and 1.4:1) were synthesized by the traditional and modified coprecipitation routes. For this latter case, the flow rate at which the reactants were contacted was set to 0.67 mL/min. The reaction time was 1 hour in all our experiments. In addition to crystal growth, cation distribution, internal magnetic field, morphology, and chemical composition, the presence of a secondary phase ($\alpha\text{-Fe}_2\text{O}_3$) by X-ray diffraction, see **Figure 6**, were identified responsible for the observed wide range of magnetic properties.

Average crystallite sizes in produced ferrite powders ranging between 11–12 nm and 15–19 nm were obtained using the conventional and the modified coprecipitation methods respectively. Excess of iron, (3:1 Fe:Co mole ratio), caused the formation of a secondary phase that was identified as hematite, $\alpha\text{-Fe}_2\text{O}_3$. In turn, less crystalline powders were obtained when the Fe:Co mole ratio was decreased from 3:1 to 1.4:1 [32].

Table 2 summarizes the nominal and experimental (measured) Fe:Co mole ratios in synthesized ferrite nanocrystals. The experimental Fe:Co mole ratios represent an average from measurements at five different regions in the sample using energy dispersive X-ray spectroscopy. For all cases, approximately 78% of the Fe present in starting solutions was incorporated into the ferrite structure.

Average crystallite sizes of cobalt ferrite synthesized without control on the flow rate were quite similar (11–12 nm). Thus, any change in magnetic properties could be attributed to the

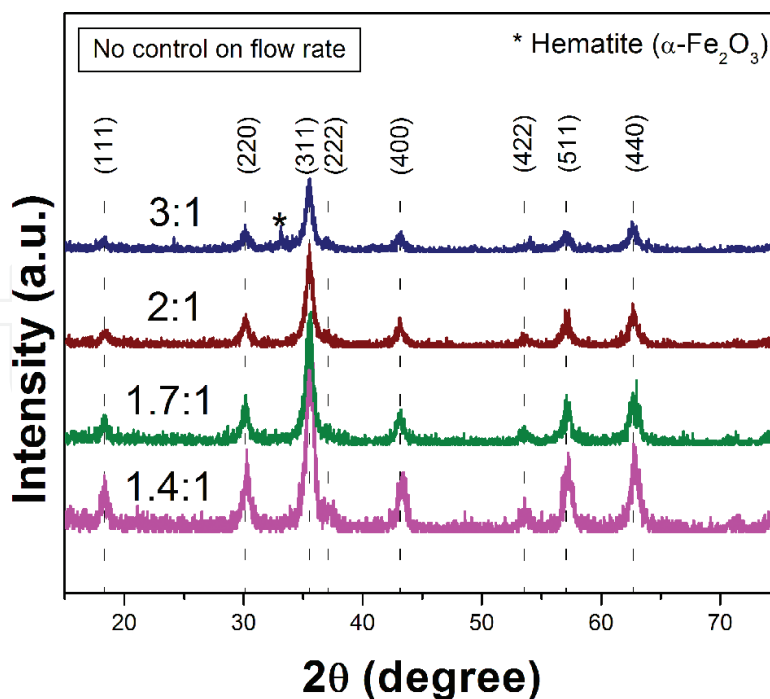


Figure 6. XRD patterns of cobalt ferrite nanocrystals synthesized without control on flow rate at different Fe:Co mole ratios. The peak with the asterisk corresponds to hematite, $\alpha\text{-Fe}_2\text{O}_3$ [32].

	No control on flow rate	Flow rate: 0.67 mL/min
Nominal Fe:Co mole ratio	Experimental Fe:Co mole ratio	Experimental Fe:Co mole ratio
3:1	2.3:1 (± 0.3)	2.3:1 (± 0.2)
2:1	1.58:1 (± 0.08)	1.54:1 (± 0.08)
1.7:1	1.31:1 (± 0.08)	1.30:1 (± 0.06)
1.4:1	1.08:1 (± 0.04)	1.0:1 (± 0.1)

Table 2. Summary of Fe:Co mole ratios of cobalt ferrite synthesized with and without control on flow rate [32].

net effect of chemical composition. For this set of samples, the highest coercivity value (548 Oe) was obtained for the sample synthesized at a 3:1 Fe:Co mole ratio. This sample is a mixture of cobalt ferrite and hematite, so surface anisotropy and interparticle interactions that contribute to the net anisotropy [33] are different when compared to pure cobalt ferrite.

Since the flow rate was kept constant in all the experiments reported in this section (0.67 mL/min), any change in the average crystallite size of the ferrite could be attributed to the variation of the chemical composition of the powders. For instance, the sample synthesized at a starting Fe:Co mole ratio of 1.7:1 yielded an average crystallite size of 18 nm, whereas it was 19 nm for the sample produced with Fe:Co mole ratio of 3:1. The corresponding coercivity magnitudes were 4412 Oe and 4249 Oe, respectively. As reported in our earlier studies, the nonstoichiometry of cobalt ferrite powders ($\text{Fe/Co} < 2$) would influence the coercivity due to the distribution of Fe ions within A- and B-sites in the spinel structure [26].

Mössbauer spectroscopy measurements help to study the Fe cationic environment and how their distribution between octahedral and tetrahedral sites changes in addition to the internal magnetic field. This technique can also elucidate whether surface effects are present. These results are presented below.

4.3.2. Influence of the Fe:Co mole ratio on the ferrite magnetic structure: Mössbauer spectroscopy measurements

The fitting of the spectra corresponding to the ferrite synthesized at a Fe:Co mole ratio of 2 and 1.7 were carried out with the hyperfine field distribution (HFD) model, considering four sites. Samples were synthesized at a flow rate of 0.67 mL/min. The doublet peaks in **Figure 7** at the central part of the Mössbauer spectra is attributed to the phenomenon of superparamagnetic relaxation, arising from particles with single domain attributes. Given the broad aspects of this component, we can confirm some distribution of particle size within this superparamagnetic fraction, with some of them having their blocking temperature close to 298 K (room temperature conditions).

The most remarkable discrepancy between the two spectra of **Figure 7** relies on both the relative abundances in each subsites, and the internal magnetic field of the octahedral and tetrahedral cationic positions. Based on the features of each Mössbauer spectrum, the superparamagnetic components in each sample was estimated to be 17% of the total material

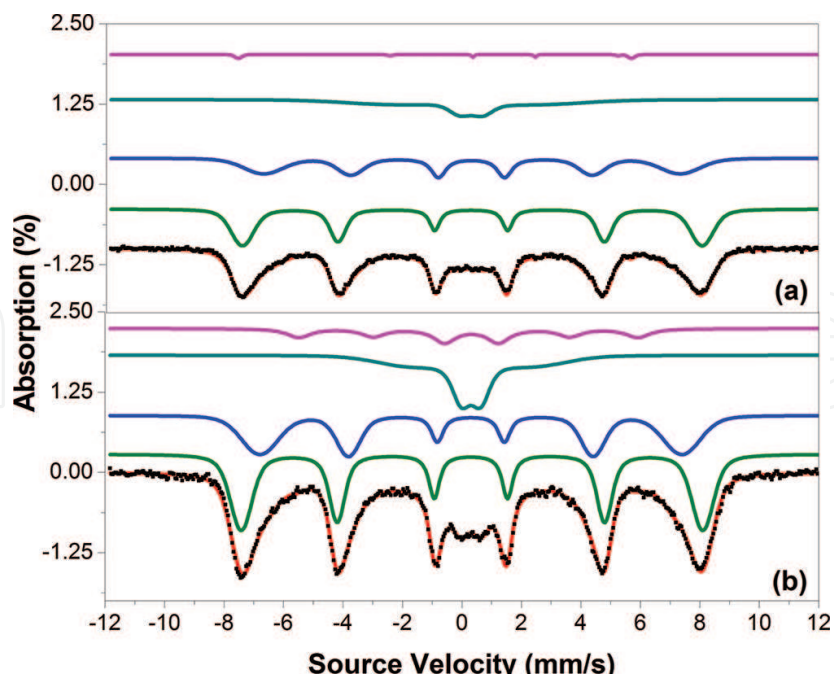


Figure 7. Fitted Mössbauer spectra corresponding to cobalt ferrite nanocrystals synthesized at 0.67 mL/min and nominal Fe:Co mole ratios of 2:1 (a) and 1.7:1 (b). The green, blue, cyan, and magenta fittings correspond to sites 1, 2, 3, and 4, respectively [32].

suggesting that the synthesis process did not affect the particle distribution. The corresponding internal magnetic field of the octahedral and tetrahedral Fe is found to be very similar in both samples. A noticeable difference between both spectra arises from the fourth component. The fourth component of the spectrum “b” (Fe:Co 1.7:1), accounted for 10% of the sample, which was very high when compared to the component but for sample “a” (Fe:Co 2:1) where it represented 0.9% of the sample. The surface cations (site-4) exhibit smaller internal magnetic field and broadened absorption lines indicating a more disordered state at the surface (spin canting) being responsible for the lack of magnetization saturation and higher coercivity value due to surface anisotropy [34].

4.3.3. Effect of the flow rate on the ferrite magnetic structure: Mössbauer spectroscopy measurements

Mössbauer spectra of cobalt ferrite nanocrystals produced at a 1.4:1 Fe:Co mole ratio with, and without control of the flow rate, were analyzed. Site-1 is attributed to Fe cations in the octahedral position of the spinel structure, while site-2 corresponds to the Fe located in the tetrahedral position.

Regarding the analysis of the spectrum corresponding to the sample synthesized without control of flow rate, the internal magnetic field values corresponding to the Fe-sites were higher than those for the powders synthesized at 0.67 mL/min. Furthermore, the relative abundance of sites-1 and 2 in the samples synthesized without control of flow rate (42.32 and 41.26%, respectively) followed an antagonistic trend when compared to the same parameters for the samples produced at 0.67 mL/min (36.80 and 42.75%); i.e., there are more Fe cations in site-1 when the powders are synthesized with no control of the flow rate. In

other words, the control of the flow rate of the addition of reactants during the synthesis of the cobalt ferrite nanocrystals affects the average crystallite size and the distribution of Fe ions within A and B sites in the spinel structure. This unexpected change in the atomic distribution should also be involved with the magnetic properties observed in those high-coercivity samples.

4.4. Inhibition of crystal growth: use of oleic acid sodium salt during the cobalt ferrite crystal formation

The use of surfactants or polymers comes from the necessity to produce extremely small particles which could help us to determine the actual superparamagnetic limit in the cobalt ferrite. Oleic acid sodium salt (Na-oleate) was used to inhibit crystal growth, because of expected surface interaction between polar groups and nanoparticles, as well as to prevent nanoparticle aggregation through strong steric interactions promoted by the adsorption of the surfactant ("capping ligand"). This surfactant has long chains that confer a physical impediment preventing particle growth and/or aggregation.

As discussed above, a reaction time as short as 5 minutes was conducive to the formation of ferrite nanocrystals in the 10–11 nm range, which suggested a very fast formation and growth of earlier ferrite nuclei. Therefore, as an attempt to avoid crystal growth, the cobalt ferrite powder was removed right after the metal solution contacted the boiling NaOH/Na-oleate solution.

The corresponding average crystallite sizes were estimated at 4 and 9 nm when the synthesis took place with and without addition of the surfactant, respectively. This result suggests that the ferrite formation was interrupted in the nucleation stage with practically no time for the nuclei to grow any further.

The extremely small crystal size was also confirmed by TEM analyses. TEM images from **Figure 8** confirmed the formation of nanocrystals with a diameter around 4 nm.

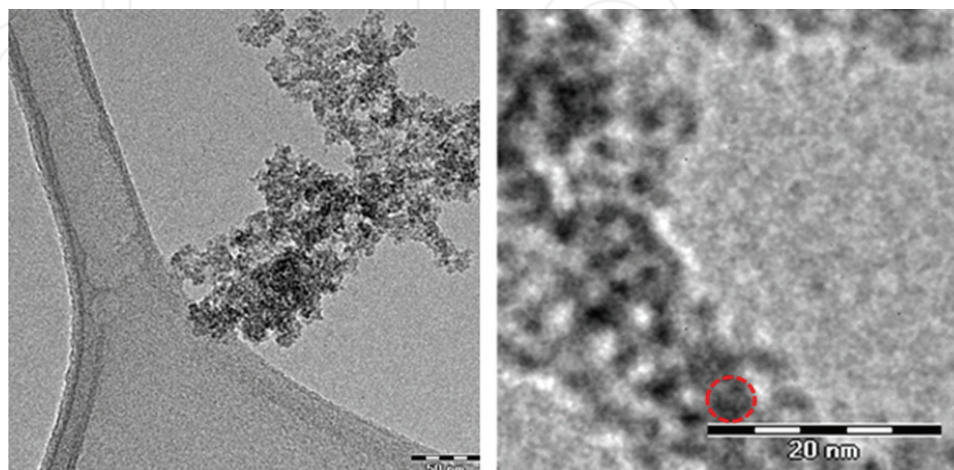


Figure 8. TEM images of cobalt ferrite nanocrystals synthesized in presence of 0.011 M Na-oleate.

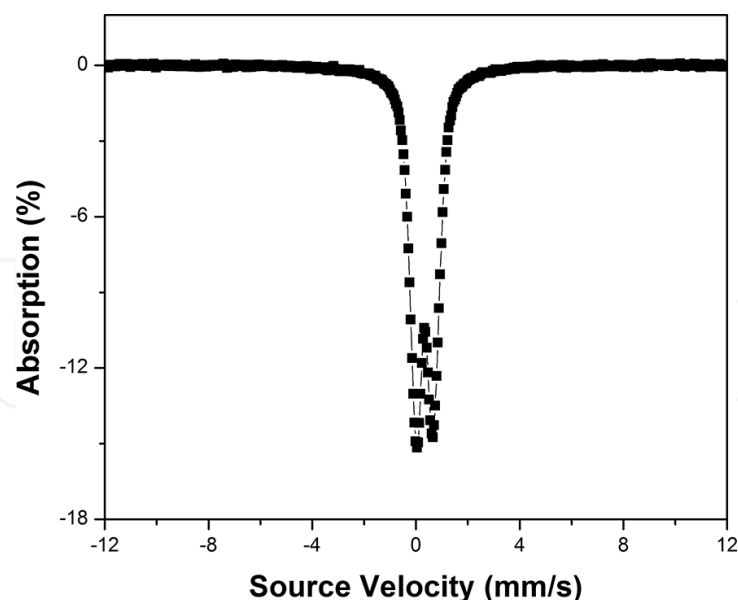


Figure 9. Mössbauer spectrum of cobalt ferrite synthesized in presence of Na-oleate.

The 9 nm nanoparticles exhibited a coercivity of 189 Oe whereas the 4 nm ones reported coercivity as low as 3 Oe. The latter value falls within the experimental error of the instrument; i.e., these particles practically did not show any coercivity.

The presence of the quadrupole splitting in the Mössbauer spectrum of the 4 nm cobalt ferrite nanocrystals (**Figure 9**) may suggest the superparamagnetic nature of the synthesized crystals. Electric quadrupole interaction occurs if at least one of the nuclear states involved possesses a quadrupole moment (which is the case for nuclear states with the spin $I > 1/2$) and if the electric field at the nucleus is inhomogeneous. In the case of ^{57}Fe , the first excited state (14.4 keV state) has a spin $I = 3/2$ and therefore also an electric quadrupole moment. It can be visualized by the precession of the quadrupole moment vector about the field gradient axis sets in and splits the degenerate $I = 3/2$ level into two substates with magnetic spin quantum numbers $mI = \pm 3/2$ and $\pm 1/2$. The energy difference between the two substates (ΔEQ) is observed in the spectrum as the separation between the two resonance lines [35]. On this basis, the superparamagnetic nature of the 4 nm nanocrystals can be proposed.

4.5. ZFC/FC measurements as a function of ferrite crystal size

In order to study the magnetic properties as a function of crystal size in more detail, cobalt ferrite nanocrystals with different crystal sizes in the 10–23 nm range were selected from previous sections. The magnetization curves of the superparamagnetic sample (4 nm in average size) were investigated in the zero-field-cooled/field-cooled (ZFC/FC) protocols using a Quantum Design SQUID unit, under an external magnetic field of 100 Oe and in the temperature range from 300 to 2 K. The powders were fixed in a solid matrix of poly(styrene-divinylbenzene) as described by Calero-Diaz del Castillo and Rinaldi [36]. The ZFC/FC profile for the

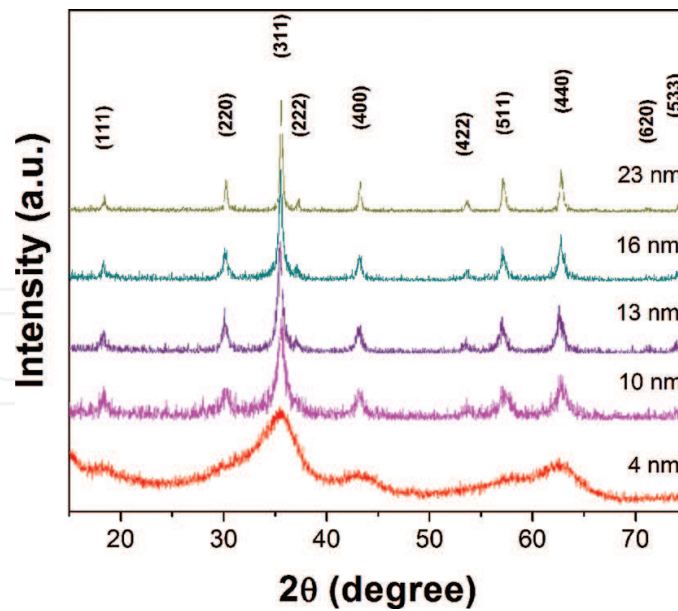


Figure 10. XRD patterns of cobalt ferrite with different average crystallite sizes.

4 nm crystals indicated they were blocked below 115 K, i.e., these nanoparticles would behave ferromagnetically below that blocking temperature [17]. As evident in Figure 10, the sharpening and intensity of the XRD peaks of cobalt ferrite powders were enhanced in those powders exhibiting larger average crystallite sizes.

Finally, the M-H loops of the different samples were also measured in the SQUID unit at 2K and 300K. As the M-H loop of Figure 11 shows, the coercivity of the 23 nm samples

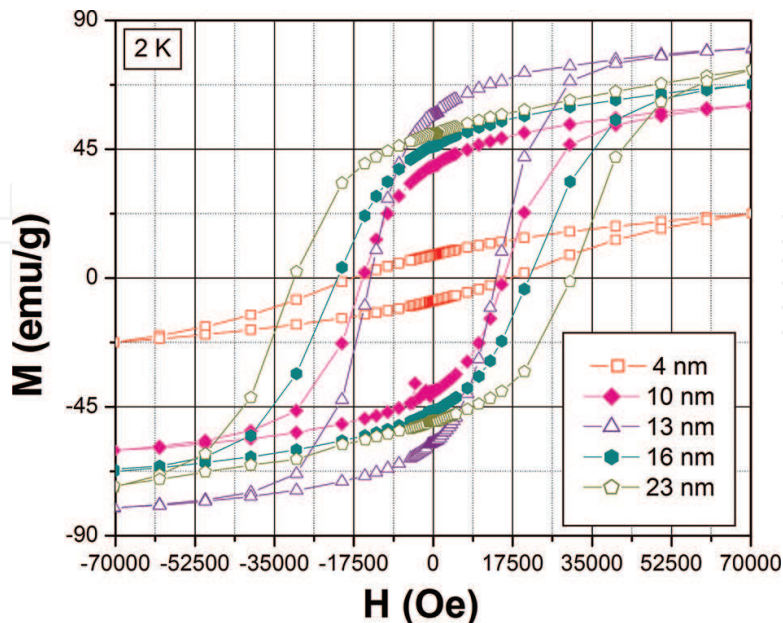


Figure 11. M-H loops at 2 K of cobalt ferrite powders with different average crystallite sizes.

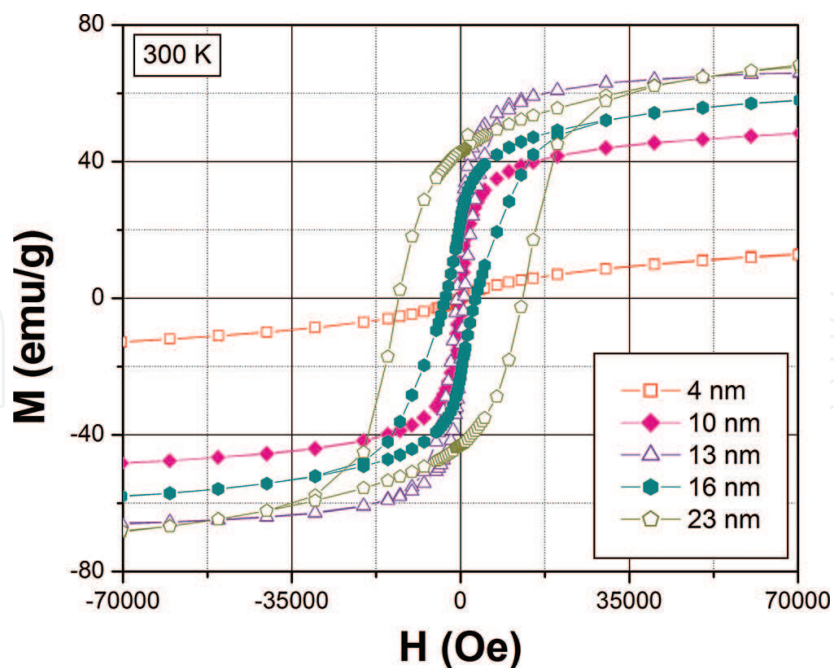


Figure 12. M-H loops at 300 K of cobalt ferrite powders with different average crystallite size.

at 2 K reached a value as high as 30 kOe. To our knowledge, this is the highest coercivity value reported for cobalt ferrite nanocrystals at 2 K. Sun et al. [37] and Meron et al. [38] reported 20 and 15 kOe, respectively, for highly monodisperse cobalt ferrite, measured at 10 K. The maximum magnetization also increases at low temperatures due to the absence of thermal energy responsible for spin rotation and randomization. The M-H loops at 2 and 300 K are shown in Figures 11 and 12. An increase in coercivity as a function of crystal size was observed as expected. Coercivity values ranged between 17–30 kOe at 2 K and 0.2–12.9 kOe at 300 K.

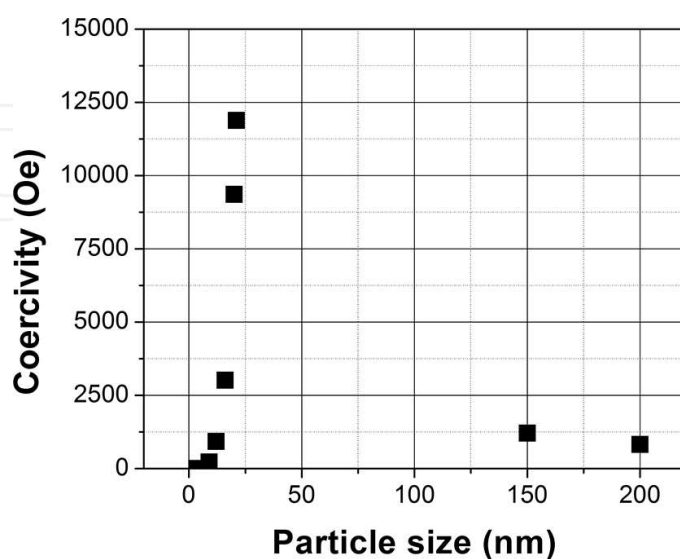


Figure 13. Variation of coercivity with particle size in cobalt ferrite particles synthesized in the present study.

4.6. Particle size dependence of coercivity revisited

In the above, the particle size dependence of the coercivity in cobalt ferrite nanocrystals has been demonstrated and discussed. Different approaches such as experimental design, size-sensitive phase separation method, and surfactants discussed above were the essential tools to obtain particles with a wide range of sizes. They helped us to achieve the main objective of this research: to determine the limits of the single-domain and multidomain regions as a function of the composition, structure, and crystal size in ferrimagnetic ferrites. It is important to notice that the theoretical coercivity values have been greatly surpassed. An experimental plot of coercivity versus particle size summarizes some of the values obtained and it is shown in **Figure 13**. Data corresponding to 150 and 200 nm were obtained using a postsynthesis thermal treatment [39].

5. Conclusions

Tuning the magnetic properties of cobalt ferrite at the nanoscale was achieved by controlling crystal size, chemical composition, and cation distribution. Average crystallite sizes ranging between 4 and 23 nm were successfully synthesized. The corresponding room temperature coercivity values varied between 3 Oe and 11.9 kOe. The 23 nm nanocrystals exhibited coercivity as high as 11.9 kOe, which is reported here for the first time. The corresponding magnetization and squareness ratio were 48 emu/g and 0.72, respectively.

The suitable combination of flow rate-controlled synthesis complemented by acid washing and magnetically assisted size-sensitive separation processes provided favorable conditions for the enhancement of nanoparticles monodispersity and tailoring of the corresponding magnetic properties. Smaller and more soluble nanocrystals that contribute negatively to coercivity (superparamagnetic particles) were selectively dissolved during the acid washing step. This selective dissolution of the superparamagnetic fraction took place in addition to the removal of the poorly crystalline layer on the surface of the nanocrystals.

The effect of the nominal Fe:Co mole ratio in starting solutions on the structural and magnetic properties of the nanocrystals was also investigated. Findings revealed that the cationic distribution in the ferrite was dependent on the nominal Fe:Co mole ratio whereas the contribution of the surface cations, and hence the surface anisotropy, became remarkable under flow rate-controlled synthesis conditions. Accordingly, the colossal coercivity attained in nanometric cobalt ferrite crystals became possible not exclusively by control of crystal size, but also through the promotion of the mentioned effects viz. surface anisotropy and atomic rearrangements of Fe species within the ferrite lattice.

About 4 nm cobalt ferrite crystals were produced using Na-oleate as a surfactant that inhibited crystal growth. The superparamagnetic behavior of these nanocrystals was confirmed by M-H measurements and Mössbauer spectroscopy techniques.

The temperature dependence of the magnetic properties of cobalt ferrite was studied as a function of crystal size. The 23 nm sample (room temperature coercivity of 11.9 kOe) reported a 2 K coercivity as high as 30 kOe.

Acknowledgements

This material is based upon work supported by The National Science Foundation under Grant No. HRD 13455156 (CREST II program).

Author details

Oscar Perales-Pérez^{1*} and Yarilyn Cedeño-Mattei^{2,3}

*Address all correspondence to: oscarjuan.perales@upr.edu

1 Department of Engineering Sciences and Materials, University of Puerto Rico, Mayagüez, Puerto Rico

2 Department of Biology, Chemistry, and Environmental Sciences, Interamerican University of Puerto Rico, San Germán, Puerto Rico

3 Department of Chemistry and Physics, University of Puerto Rico, Ponce, Puerto Rico

References

- [1] Sun C, Lee JS, Zhang M. *Adv. Drug Delivery Rev.* 2008;**60**:1252–1265.
- [2] Arulmurugan R, Vaidyanathan G, Sendhilnathan S, Jeyadevan BJ. *Magn. Mater.* 2006;**298**:83–94.
- [3] Terzzoli MC, Duhalde S, Jacobo S, Steren L, Moina CJ. *Alloys Compd.* 2004;**369**:209–212.
- [4] Song Q, Zhang ZJ. *J. Am. Chem. Soc.* 2004;**126**:6164–6168.
- [5] Hyeon T, Chung Y, Park J, Lee SS, Kim Y, Park BH. *J. Phys. Chem B.* 2002;**106**:6831–6833.
- [6] Khedr MH, Omar AA, Abdel-Moaty SA. *Colloids Surf. A.* 2006;**281**:8–14.
- [7] Li S, John VT, O'Connor C, Harris V, Carpenter EJ. *Appl. Phys.* 2000;**87**:6223–6225.
- [8] Berkowitz AE, Schuele WJ. *J. Appl. Phys.* 1959;**30**:S134.
- [9] Neel L. *C.R. Acad. Sci. Paris.* 1947;**224**:1488–1490.
- [10] Goldman A. *Modern Ferrite Technology.* New York: Van Nostrand Reinhold; 1990.
- [11] Callister Jr. W. *Materials Science and Engineering an Introduction.* 6th ed. New Jersey: John Wiley & Sons Inc.; 2003.
- [12] Luborsky FE. *J. Appl. Phys.* 1961;**32**:S171.
- [13] O'Handley RC. *Modern Magnetic Materials: Principles and Applications.* 1st ed. New York: Wiley Interscience; 1999.

- [14] Bedanta S, Kleemann WJ. *Phys. D: Appl. Phys.* 2009;**42**:013001.
- [15] Stoner EC, Wohlfarth EP. *Trans. R. Soc. Lond. A.* 1948;**240**:599–642.
- [16] Chinnasamy C, Jeyadevan B, Perales-Perez O, Shinoda K, Tohji K, Kasuya A. *IEEE Trans. Magn.* 2002;**38**:2640–2642.
- [17] Perales-Perez O, Sasaki H, Kasuya A, Jeyadevan B, Tohji K, Hihara T, Sumiyama K. *J. Appl. Phys.* 2002;**91**:6958–6960.
- [18] Moumen N, Bonville P, Pileni MP. *J. Phys. Chem.* 1996;**100**:14410–14416.
- [19] Cedeño-Mattei Y, Perales-Perez O, Tomar MS, Roman F, Voyles PM, Stratton WG. *J. Appl. Phys.* 2008;**103**:07E512.
- [20] Sileo EE, Garcia-Rodenas L, Paiva-Santos CO, Stephens PW, Morando PJ, Blesa MA. *J. Solid State Chem.* 2006;**179**:2237–2244.
- [21] Letellier P, Mayaffre A, Turmine M. *J. Phys. Condens. Matter.* 2007;**19**:436229.
- [22] Figueroa CA, Sileo EE, Morando PJ, Blesa MA. *J. Colloid Interface Sci.* 2000;**225**:403–410.
- [23] Sawatzky GA. *J. Appl. Phys.* 1968;**39**:1204–1205.
- [24] Manova E, Kunev B, Paneva D, Mitov I, Petrov L, Estournès C, D'Orléan C, Rehspringer J, Kurmoo M. *Chem. Mater.* 2004;**16**:5689–5696.
- [25] Zhao L, Zhang H, Xing Y, Song S, Yu S, Shi W, Guo X, Yang J, Lei Y, Cao F. *J. Solid State Chem.* 2008;**181**:245–252.
- [26] Cedeño-Mattei Y, Perales-Perez O, Uwakweh ONC, Xin Y. *J. Appl. Phys.* 2010;**107**:09A741.
- [27] Olsson RT, Salazar-Alvarez G, Hedenqvist MS, Gedde UW, Lindberg F, Savage S. *J. Chem. Mater.* 2005;**17**:5109–5118.
- [28] Globus A, Monjaras R. *IEEE Trans. Magn.* 1975;**11**:1300–1302.
- [29] Salazar-Alvarez G, Olsson RT, Sort J, Macedo WAA, Ardisson JD, Baró MD, Gedde UW, Nogués J. *Chem. Mater.* 2007;**19**:4957–4963.
- [30] Henderson CMB, Charnock JM, Plant DA. *J. Phys. Condens. Matter.* 2007;**19**:076214.
- [31] Töpfer J, Dieckmann R. *J. Eur. Ceram. Soc.* 2004;**24**:603–612.
- [32] Cedeño-Mattei Y, Perales-Perez O, Uwakweh ONC. *Mat. Chem. Phys.* 2012; **132**: 999–1006.
- [33] Xu P, Han X, Zhao H, Liang Z, Wang J. *Mater Lett.* 2008;**62**:1305–1308.
- [34] Papaefthymiou GC. *Nano Today.* 2009;**4**:438–447.
- [35] Miller JS, Drillon M. *Magnetism: Molecules to Materials.* New York: Wiley-VCH; 2003.
- [36] Calero-Diaz del Castillo VL, Rinaldi C. *IEEE Trans. Magn.* 2010;**46**:852–859.

- [37] Sun S, Zeng H, Robinson DB, Raoux S, Rice PM, Wang SX Li G. *J. Am. Chem. Soc.* 2004;**126**:273–279.
- [38] Meron T, Rosenberg Y, Lereah Y, Markovich G. *J. Magn. Magn. Mater.* 2005;**292**:11–16.
- [39] Cedeño-Mattei Y, PhD Dissertation, University of Puerto Rico: Mayaguez Campus, 2011.

IntechOpen

IntechOpen